## **Cornea & External Disease**

# Anatomical Region-Specific Transcriptomic Signatures and the Role of Epithelial Cells in Pterygium Inflammation: A Multi-Omics Analysis

Chaerim Song<sup>1,\*</sup>, Seokho Myung<sup>1,2,\*</sup>, Hanseul Cho<sup>1,2,\*</sup>, Tae Gi Kim<sup>3</sup>, Soohyun Chun<sup>1,2</sup>, Minju Seo<sup>1,2</sup>, Hyunmin Yu<sup>1,2</sup>, Seoyeon Kim<sup>1</sup>, Ye-Ah Kim<sup>1,4</sup>, Junghyun Kim<sup>5</sup>, Jaeyong Shin<sup>6</sup>, Sungsoo Bae<sup>7</sup>, Yoonsung Lee<sup>1</sup>, Min Seok Kang<sup>8</sup>, and Man S. Kim<sup>1</sup>

- <sup>1</sup> Translational-Transdisciplinary Research Center, Clinical Research Institute, Kyung Hee University Hospital at Gangdong, College of Medicine, Kyung Hee University, Seoul, Republic of Korea
- <sup>2</sup> Department of Medicine, Kyung Hee University College of Medicine, Seoul, Republic of Korea
- <sup>3</sup> Department of Ophthalmology, Kyung Hee University College of Medicine, Kyung Hee University Hospital at Gangdong, Seoul, Republic of Korea
- <sup>4</sup> Department of Biomedical Science and Technology, Graduate School, Kyung Hee University, Seoul, Republic of Korea
- <sup>5</sup> Division of Tourism & Wellness, Hankuk University of Foreign Studies, Yongin-si, Gyeonggi-do, Korea
- <sup>6</sup> Department of Preventive Medicine, Yonsei University College of Medicine, Seoul, Republic of Korea
- <sup>7</sup> Department of Neurosurgery, Kyung Hee University Hospital at Gangdong, Kyung Hee University College of Medicine, Seoul, Republic of Korea
- <sup>8</sup> Department of Ophthalmology, Kyung Hee University Hospital, College of Medicine, Kyung Hee University, Seoul, Republic of Korea

Correspondence: Min Seok Kang, Department of Ophthalmology, Kyung Hee University Hospital, College of Medicine, Kyung Hee University, 26, Kyungheedae-ro, Dongdaemun-gu, Seoul 02447, Republic of Korea. e-mail: nietzsche@khu.ac.kr

Man S. Kim,

Translational-Transdisciplinary Research Center, Clinical Research Institute, Kyung Hee University Hospital at Gangdong, College of Medicine, Kyung Hee University, 26, Kyungheedae-ro, Dongdaemun-gu, Seoul 02447, Republic of Korea. e-mail: manskim@khu.ac.kr

Received: February 24, 2025 Accepted: June 15, 2025 Published: August 7, 2025

**Keywords:** pterygium; inflammation; energy metabolism; multi-omics; RNA-sequencing

**Purpose:** This study aims to understand the differences in cellular and molecular patterns between the Main and Accessory (Acc) regions of pterygium tissue, with a focus on inflammation and mitochondrial energy metabolism.

**Methods:** We collected bulk RNA sequencing (RNA-seq) data from six pterygium patients and single-cell RNA-seq data from two pterygium patients. Subsequently, we investigated pathway enrichment, pathway correlation, differential gene expression, protein-protein interactions, and cell-cell communication in pterygium.

**Results:** Bulk RNA-seq analysis revealed distinct expression patterns in the Acc group compared to the Main and control groups. This finding suggested the need to separate the Main and Acc regions within pterygium samples and use single-cell data to understand differences between the Main and control groups that bulk data could not capture. The single-cell data identified a cluster of epithelial cells containing only pterygium samples, which contributed significantly to the ANGPTL, IL1, and KLK signaling networks. Cells involved in inflammatory pathways associated with the integrated stress response and the renin-angiotensin-aldosterone system, both of which exhibited high correlations with energy metabolism-associated pathways, were significantly upregulated. Additionally, expression changes in multiple proinflammatory, antioxidant, and immune-associated genes were identified.

**Conclusions:** The distinctions between the Main and Acc groups suggest the necessity of distinguishing anatomical regions in future pterygium studies. Additionally, the pivotal role of epithelial cells from the Main group in the inflammation of pterygium indicates a potential clinical approach for managing the disease.

**Translational Relevance:** This study aims to identify apex-specific biomarkers of pterygium for a more efficient diagnosis and treatment.

Copyright 2025 The Authors tvst.arvojournals.org | ISSN: 2164-2591



Citation: Song C, Myung S, Cho H, Kim TG, Chun S, Seo M, Yu H, Kim S, Kim YA, Kim J, Shin J, Bae S, Lee Y, Kang MS, Kim MS. Anatomical region-specific transcriptomic signatures and the role of epithelial cells in pterygium inflammation: A multi-omics analysis. Transl Vis Sci Technol. 2025;14(8):13, https://doi.org/10.1167/tvst.14.8.13

#### Introduction

Ptervgium is characterized by a triangular, wedgeshaped fibrovascular growth extending from the conjunctiva onto the cornea. Rather than being a purely degenerative lesion, it is now understood as a proliferative disorder involving a hyperplastic, centripetally directed growth of altered limbal epithelial cells, accompanied by Bowman's layer dissolution, epithelial-mesenchymal transition, and an activated fibroblastic stroma with inflammation, neovascularization, and extracellular matrix remodeling, all mediated by the concerted actions of cytokines, growth factors, and matrix metalloproteinases.<sup>1,2</sup> A defining pathological feature is focal limbal stem cell dysfunction. In our previous study, we demonstrated that intrinsic gene regulatory mechanisms are closely linked to the inflammatory responses in pterygium using RNA sequencing, and we further identified differences in gene regulatory patterns between Asian and European ethnic groups.<sup>3</sup>

Although surgical excision is commonly performed to manage pterygium,<sup>4</sup> recurrence—characterized by the regrowth of fibrovascular tissue across the limbus—remains a major clinical challenge. In addition to surgery, topical medical therapies such as cyclosporine have shown efficacy, particularly through their anti-inflammatory effects.<sup>5,6</sup> Given that inflammation plays a central role in pterygium pathogenesis, medical approaches targeting inflammatory pathways are of increasing interest and highlight the need for further molecular and translational research in this area.

The anatomic characteristics of pterygium affect the treatment method and its success rate. The anatomy of pterygium can be divided into three parts: head, neck, and body. The invading portion growing toward the center of the cornea, which contains the apex of the tissue is called the head. Pterygium is firmly adherent to the cornea and is characterized by disruption of Bowman's layer, along with alterations in the overlying epithelium, which may ultimately impair vision. The communicating part between the body and the head, which overlies the limbus, is the neck. The conjunctival portion with a base toward the medial canthus is known as the body. The likelihood of recurrence is high if the head of the pterygium is not completely

removed during surgery. If the body of pterygium is not adequately managed, the risk of recurrence increases as well. These points suggest that the pathogenesis of pterygium may differ based on its anatomical regions.

This study aims to provide a considerable understanding of pterygium-associated pathogenesis and identify potential therapeutic targets through bulk and single-cell RNA sequencing (scRNA-seq) data analyses. We applied various analytical approaches, including enrichment analyses and cell-cell communication analysis across different cell types of pterygium. Specifically, we investigated the differences between the anatomical parts of the pterygium and explored factors that may influence the onset and recurrence of pterygium.

# **Methods**

#### **Sample Collection**

Each of the Main, Acc, and Normal samples of the bulk RNA-seq data was collected from six primary pterygium patients by elective pterygium excision, approved by Kyung Hee University Hospital at Gangdong (IRB No. 2022-04-006). The patients, aged 61 to 72, included three males and three females. For bulk RNA-seq data, the head and neck of the pterygium were collected and denoted as Main, whereas the body of the pterygium was denoted as Acc. The normal conjunctival tissue from each patient was collected as a control, denoted as Normal. The samples were transferred to 2 mL Eppendorf tubes (Eppendorf, Hamburg, Germany) and stored at  $-80^{\circ}$ C for subsequent total RNA extraction.

ScRNA-seq data was collected by Kyung Hee University Hospital at Gangdong using the Chromium Next GEM Single Cell 3' RNA library kit (v3.1). The Main and Normal samples were collected from each of the two pterygium patients in the dataset. The samples were immediately transferred to 2 mL Eppendorf tubes (Eppendorf, Hamburg, Germany) containing MACS Tissue Storage Solution (Cat: 130-100-008, Miltenyi Biotec, Bergisch Gladbach, Germany) and packed on ice.

#### **RNA-Sequencing**

For bulk RNA sequencing, total RNA was extracted from the tissue samples using standard protocols, followed by DNase treatment to remove DNA contamination. For mRNA profiling, an mRNA purification kit was used, whereas a ribo-zero rRNA removal kit was used for studies including non-coding RNA. The purified RNA underwent random fragmentation for short-read sequencing. These fragments were reverse transcribed into cDNA, and distinct adapters were ligated to both ends. The library was PCR-amplified to obtain sufficient quantities for sequencing and underwent size selection for inserts of 200-400 base pairs. Paired-end sequencing was then conducted with a read length appropriate for the study design. For the scRNA-seq data, the Chromium Single Cell 3' Protocol was used to analyze 3' digital gene expression of 500 to 10,000 individual cells per sample. Single cells, reagents, and Gel Beads with barcoded oligonucleotides were encapsulated into nanoliter-scale Gel Beads-in-emulsion (GEMs) using Next GEM Technology. This method allowed the indexing of each cell's transcriptome and cell surface protein with approximately 3,500,000 unique 10x Barcodes. Within GEMs, poly-adenylated mRNA was captured by poly(dT) primers, resulting in barcoded, full-length cDNA synthesis. The resulting Single Cell 3' gene expression and feature barcode libraries were sequenced on the Illumina system, using pairedend sequencing to read both ends of the cDNA fragments.

# **Data Preprocessing**

For bulk RNA-seq data, FASTQC (v0.11.7) was used to check the quality of the data, and STAR (v2.7.3a) and HTSeq-Count (v0.12.4) were used to map the reads to the reference genome, GRCH38. The data was normalized using the rlog (regularized log) transformation from the DESeq2 package (v1.44.0). For scRNA-seq data, FASTQC (v0.11.7) was performed on the raw sequences for a quality check. The FASTQ files were preprocessed through 10x Genomics Cloud Analysis by choosing Next GEM Single Cell 3' Gene Expression as the library type and setting checkLibraryCompatibility to true, Chemistry to auto, createBam to false, disableAbAggregateDetection to false, includeIntrons to true, and noSecondaryAnalysis to false. The resulting genebarcode matrix output was downloaded as a Market Exchange file format. The Seurat R package (v5.1.0) was used to perform integration. The data was filtered to those with less than 9000 genes detected per cell

and less than 10,000 unique molecular identifiers per cell. The data was normalized with the NormalizeData function using the LogNormalize method, and anchor-based canonical correlation analysis integration was applied through the IntegrateLayers function. The raw and processed RNA-seq datasets will be provided by the authors upon reasonable request.

#### **Cell Type Annotation**

The Seurat package (v5.1.0) was used to generate clusters of the cells. After testing for canonical marker expressions for a range of clustering resolution values (0.3-1.2), FindNeighbors and FindClusters were performed with a resolution of 0.6. The first 12 principal components (PCs) were chosen based on the results of the elbow plot and the heatmap of the top 20 PCs. Cell types were manually assigned to each cell cluster by matching the expressions of genes with markers from Zhang et al. and the cell atlas of the human ocular anterior segment from the Broad Institute. 10 The FindMarkers function was used to further identify and confirm the differentially expressed genes (DEGs) between different clusters. FeaturePlot and VlnPlot were also called to visually confirm the marker expressions in each cluster.

## **Differential and Enrichment Analysis**

The differential gene expression within the bulk RNA-seq data was analyzed by performing principal component analysis (PCA) and EnhancedVolcano using the DESeq2 package (v1.44.0). The plotPCA function's default value of the top 500 genes of highest variance was used to perform PCA. A P value cutoff of 0.05 and a log fold change cutoff of 1 were used to limit the DEGs to those that best represent meaningful changes in expression. The enrichGO function from the clusterProfiler R package (v4.13.3) was performed to search for enriched functional pathways. The top 10 common pathways were identified from each comparison group (Main vs. Acc, Normal vs. Acc) and were merged as a bubble plot. Protein-protein interaction (PPI) was also depicted by STRING using K-means clustering with the top 1000 DEGs. Gene ontology was used to identify the biological processes associated with cluster 1 from the PPI of both comparison groups. For enrichment analysis such as fGSEA and gene expression profile heatmaps, multiple gene lists were applied. A custom-made core inflammatory gene list obtained from Topper et al. 11 was used for inflammatory-associated analysis. For mitochondrial energy metabolism-associated analysis, a customized

core gene list acquired from Guarnieri et al. for heatmap and MitoCarta3.0 gene list for enrichment analysis (i.e., fGSEA) were used.<sup>12</sup>

#### **Correlation Analysis**

The correlation between the inflammatory and energy pathways was computed using the Van Der Waerden test. After testing multiple cutoff values, the results from fGSEA were filtered to those with P values <0.3 to ensure the inclusion of moderate enrichment signals while limiting the results to relevant pathways. The results from the Van Der Waerden test were filtered to those with P values >0.9 and the number of observations >3.

#### **Cell-Cell Communication Analysis**

The CellChat R package (v2.1.2) was used to compare the interactions between cell types in the pterygium and control samples. The interactions were limited to those associated with inflammation from CellChatDB. ComputeCommunProb was used with the type as truncatedMean and the trim as 0.05. Communications with less than 10 cells in each cell group were filtered out using filter Communication.

## Results

Because no prior study has examined the gene expression profiles of pterygium across different anatomic regions, we categorized the pterygium samples into Main (head and neck) and Acc (body) as shown in Figure 1A. We first identified significant DEGs (P value cutoff of 0.05 and a log fold change cutoff of 1) among the Main, Acc, and Normal. A relatively higher number of DEGs (4436 in Main vs. Acc; 4180 in Normal vs. Acc) were found when Main and Normal were analyzed against Acc, compared to the 115 DEGs found in Main vs. Normal (Fig. 1B). The PCA plot also revealed a clear separation of sample points between Acc and the other two groups, suggesting the presence of distinct genetic expression patterns between the Acc and Main regions (Fig. 1C). This finding points out the need for the separation of pterygium regions, unlike previous studies that analyzed the Acc and Main regions as a single group. 13

To assess whether the identified DEGs are linked to functions documented in previous studies, we conducted a Gene Ontology (GO) analysis (Fig. 1D). Pathways including synapse organization, epithelium

morphogenesis, and cell junction assembly, commonly known to be related to organ and system development, were significantly enriched in both Main and Normal relative to Acc.

To explore the functional roles of DEGs enriched in Main and Normal compared to Acc at the proteomic level, we analyzed PPI networks using STRINGdb. A prominent cluster associated with organ development emerged in the comparison of Main and Acc (Fig. 1E). The PPI comparing Normal and Acc also displayed a major cluster associated with system development. These observations are consistent with the findings from the GO analysis, highlighting the distinction between Acc and Main and similar characteristics between Main and Normal.

Inflammation and oxidative stress are key factors in the pathology of pterygium.<sup>3</sup> To further investigate the association between the inflammatory modules and anatomical region, the normalized enrichment score (NES) was computed for each module using Fast Gene Enrichment Analysis (fGSEA) with a customized inflammatory gene list obtained from Topper et al.<sup>11</sup> Most inflammatory modules were generally upregulated in Main and Normal compared to Acc (Fig. 2A). Specifically, Interleukins in Adaptive Immunity, Complement Activation/Fibrin Deposition, and the AGT Regulator Axis in the Renin-Angiotensin-Aldosterone System (RAAS) were downregulated in both Main and Normal.

Given the critical role of mitochondrial energy metabolism in inflammation and oxidative stress, we further examined gene group activation levels of mitochondrial energy metabolism-associated pathways in Acc using MitoCarta3.0 (Fig. 2B). 14,15 Consistent with the inflammatory profile, most mitochondrial energy metabolism-associated modules, including oxidative phosphorylation (OXPHOS), mitochondrial central dogma (MCD), mitochondrial dynamics and surveillance, signaling, protein import, and homeostasis, were upregulated in Main and Normal compared to Acc. Most metabolism-associated modules were also upregulated in the two groups except for the modules involved in pyruvate metabolism, xenobiotic metabolism, the urea cycle, glycine metabolism, choline and betaine metabolism, and the amidoxime-reducing complex. The clear distinction between Acc and Main and the relatively similar regulation patterns between Main and Normal suggest that the anatomical region of the samples is highly implicated in its transcriptional profile, pointing to the need to separate Acc and Main in future studies.

To provide an overview of the molecular and cellular landscape of patient-matched selective pterygium samples and normal samples, we processed

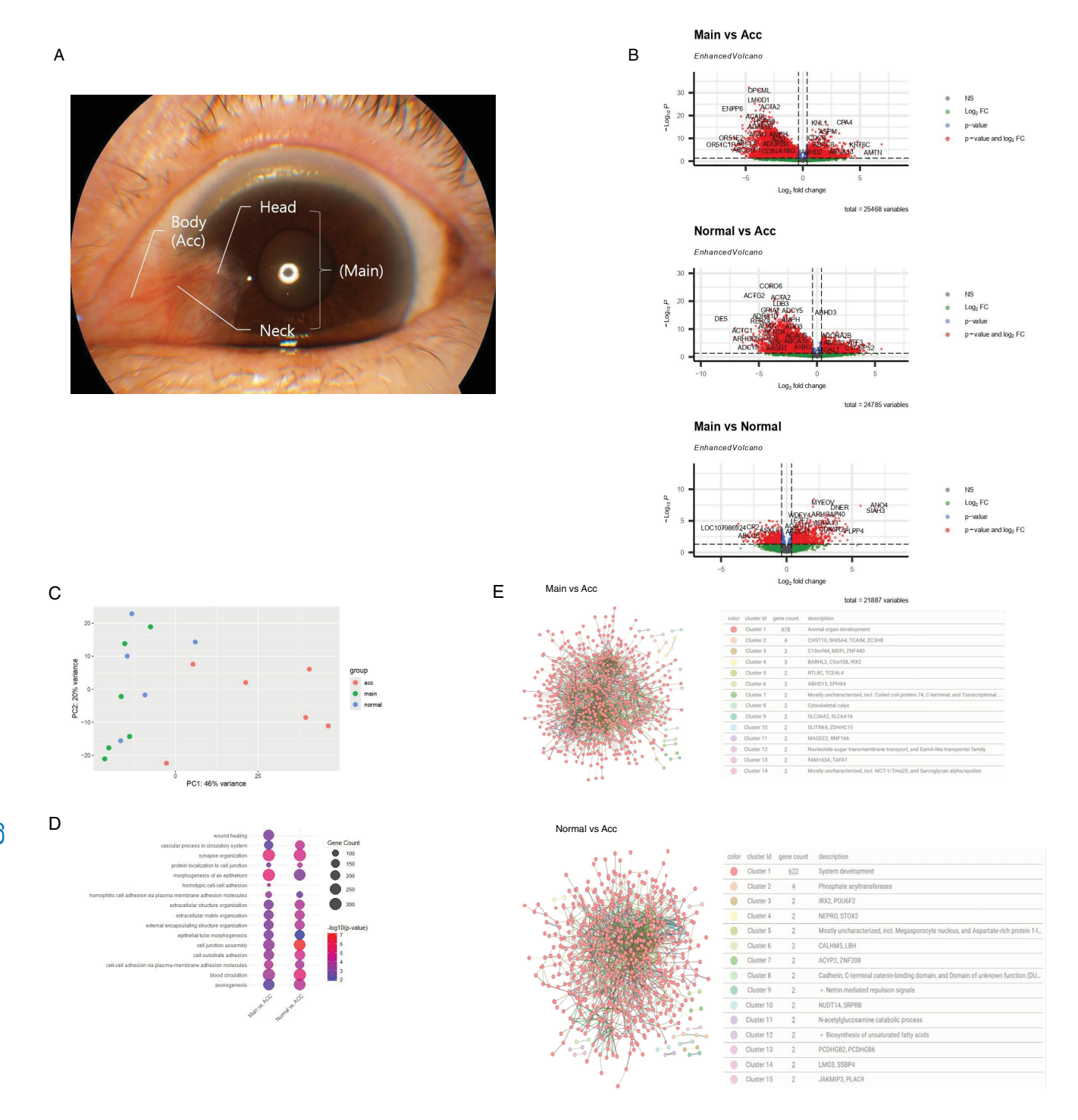


**Figure 1.** (**A**) Photo of an eye affected by pterygium. (**B**) Volcano plots of DEGs from pairwise comparisons among the Main, Normal, and Acc groups (P < 0.05,  $\log^2$  fold-change > 0.38). (**C**) PCA plot of PC1 and PC2 showing separation of Acc group from the Main and Normal groups. (**D**) Most commonly enriched pathways from GO analysis. (**E**) PPI networks with top 1000 significant DEGs.

scRNA-seq using freshly resected pterygium samples and their adjacent control (cornea) samples from two patients. Based on the distinct transcriptional patterns we identified between the anatomical regions of pterygium, we selectively collected the Main samples (non-ACC) to represent pterygium. The samples were integrated using joint analysis of heterogeneous samples (Fig. 3A).

Using marker genes from Zhang et al., <sup>10</sup> we identified seven distinct clusters of cell types, includ-

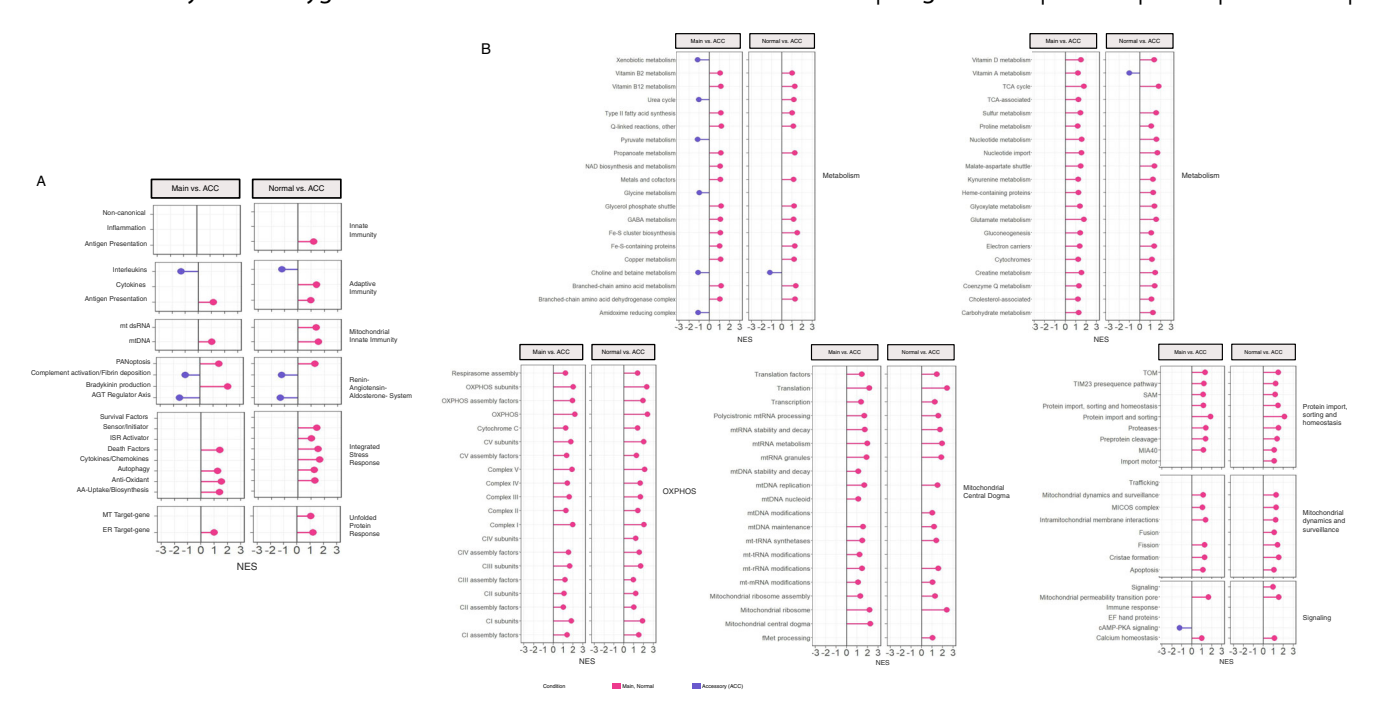
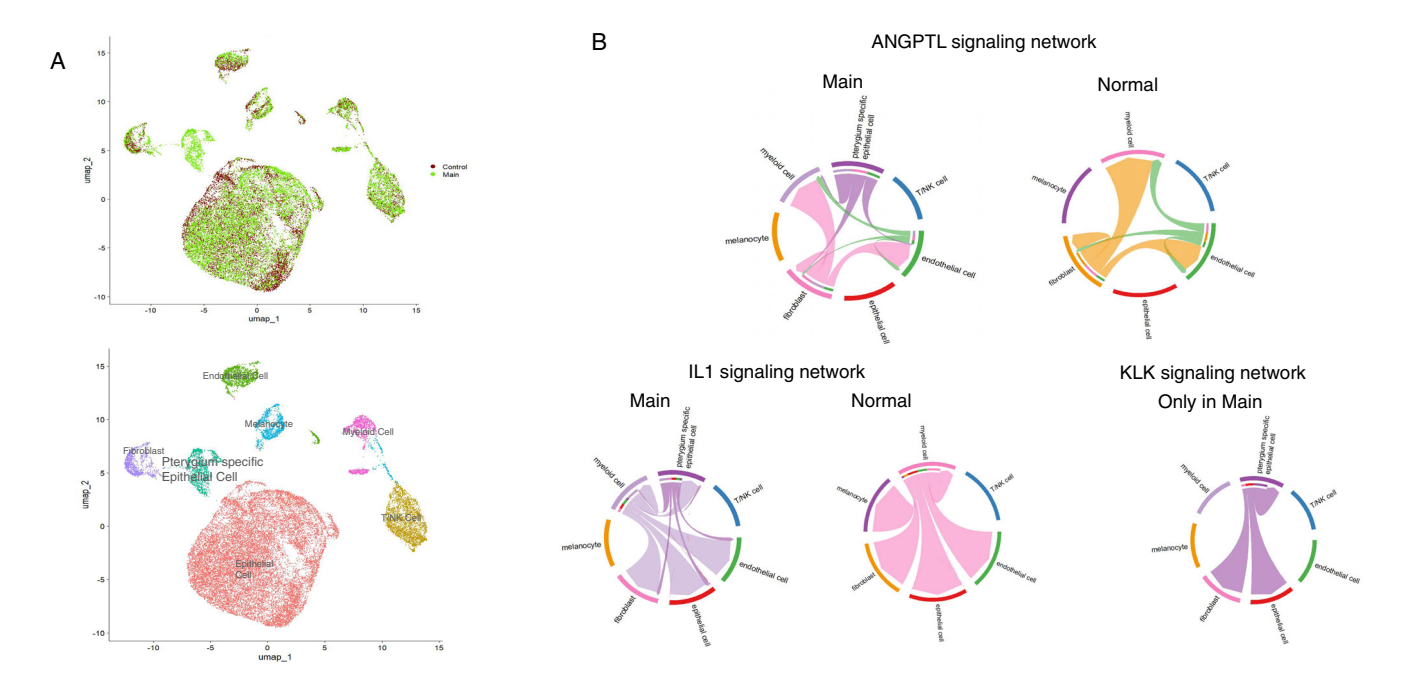


Figure 2. Lollipop plots of gene modules comparing the Acc group with the Main or Normal groups using NESs. (A) Lollipop plot of inflammatory modules. (B) Lollipop plots of mitochondrial energy metabolism-associated modules.



**Figure 3.** (**A**) Clustering of integrated data (*left*) and clusters annotated by their cell types (*right*). (**B**) Cell-cell communication of inflammatory signaling networks showing significant contributions of pterygium-specific epithelial cells in the interactions between cell types.

ing epithelial cells (KRT7, KRT5, KRT19), endothelial cells (RAMP3, VWF, PECAM1), fibroblasts (COL1A1, COL1A2, DCN), T/NK cells (TRAC, CD3E, CD3D), myeloid cells (CD68, LYZ, TYROBP), and melanocytes (TYRP1, PMEL, MLANA). Note that we identified a cluster that only consisted of ptery-

gium samples among the cells annotated as epithelial cells and denoted the group separately as pterygium-specific epithelial cells. This indicates that this cluster may be unique to or highly associated with the Main group and likely plays a role in the pathology of pterygium.

To examine the differential communication patterns among cell types in Main and Normal samples at the cellular level, we analyzed the interactions between cell types within various inflammation-associated signaling networks using CellChat. Pterygium-specific epithelial cells significantly contributed to the inflammatory response in pterygium through the ANGPTL, IL1, and KLK signaling networks (Fig. 3B). Fibroblasts, myeloid cells, endothelial cells, and epithelial cells unveiled interactions with pterygium-specific epithelial cells in these pathways.

To estimate the activation levels of inflammatory modules in each cell type, we computed their corresponding NESs through fGSEA using a customized inflammatory gene list from Topper et al. 11 (Fig. 4A). The epithelial cells in pterygium samples were upregulated in surface marker/receptor signaling in adaptive immunity and inflammation in innate immunity, whereas the canonical pathways in innate immunity were upregulated in both the epithelial and ptervgiumspecific epithelial cells. Unlike the epithelial cells found in both pterygium and control, pterygiumspecific epithelial cells were significantly upregulated in pathways involved in antioxidant responses and AA-uptake/biosynthesis from the Integrated Stress Response (ISR), as well as in complement activation/fibrin deposition and bradykinin production from the RAAS (Fig. 4A). RAAS is associated with retinal vasculopathy and inflammation, suggesting that it may be one of the pathways that the ptervgium-specific epithelial cells contribute to in the pathology of pterygium. 16

In T/NK cells, interleukin activity in adaptive immunity and most RAAS modules were upregulated in pterygium. Endothelial cells exhibited upregulation of surface marker/receptor signaling in adaptive immunity. Fibroblasts indicated increased ISR inhibitor and AA-uptake/biosynthesis in the ISR. Interleukin activity in adaptive immunity as well as survival factors and cytokines/chemokines in the ISR were activated in melanocytes. In myeloid cells, surface markers and cytokines in adaptive immunity, both non-canonical and canonical modules in innate immunity, AA-uptake/biosynthesis in the ISR, and the AGT regulator axis in the RAAS were all upregulated (Fig. 4A).

To elucidate energy-associated functional mechanisms contributing to the upregulated inflammatory modules, we analyzed the correlation between inflammatory-associated modules and mitochondrial energy metabolism-associated modules using NES values (Fig. 4B). Considering the heterogeneity of variances of module activation levels across two distinct functional categories, we employed a non-

parametric method, Van der Waerden test, to approximate the correlation. Inflammatory modules that exhibited significant correlations with the mitochondrial energy metabolism-associated modules included interleukins and surface marker receptor signaling in extracellular immunity, hyaluronan accumulation of the RAAS, antigen presentation involved in innate immunity, endoplasmic reticulum pathways of unfolded protein response, and death factors and sensor/initiator pathways of ISR. Likewise, the mitochondrial energy metabolism-associated modules that demonstrated significant correlations with the inflammatory pathways turned out to be several metabolism-associated pathways (i.e., xenobiotic metabolism, glycine metabolism, itaconate metabolism, NAD biosynthesis and metabolism, vitamin A metabolism, metals and cofactors, and nucleotide metabolism), mtRNA metabolism in the MCD, and CIV subunits and Complex I pathways of OXPHOS.

The inflammatory modules that unveiled the highest correlation were AA-uptake/biosynthesis in the ISR connected to six energy-associated nodes, followed by bradykinin production in the RAAS connected to five. These two modules were upregulated in the pterygium-specific epithelial cells, suggesting that these cells are potentially implicated in the inflammatory responses highly correlated with the mitochondrial energy metabolism of pterygium tissues. Fibroblasts and myeloid cells were also upregulated in AA-uptake/biosynthesis, while T/NK cells were upregulated in bradykinin production (Fig. 4A).

To estimate the activation levels of mitochondrial energy metabolism-associated modules in each cell type, we also computed their corresponding NESs through fGSEA using MitoCarta3.0 (Fig. 5). OXPHOS and MCD pathways were generally downregulated in pterygium. The metabolism-associated modules, however, were upregulated, suggesting the metabolic reprogramming toward metabolism-associated pathways/modules in pterygium.

Metabolism-associated modules upregulated in the pterygium-specific epithelial cells included choline and beta metabolism, vitamin metabolism, vitamin A metabolism, type II fatty acid synthesis, selenoproteins, and kynurenine metabolism. Fibroblasts of pterygium samples showed up regulations in creatine metabolism, vitamin A metabolism, urea cycle, serine metabolism, phospholipid metabolism, and nucleotide metabolism. Melanocytes were upregulated in GABA metabolism, electron-carriers, creatine metabolism, vitamin metabolism, vitamin B1 metabolism, Q-linked

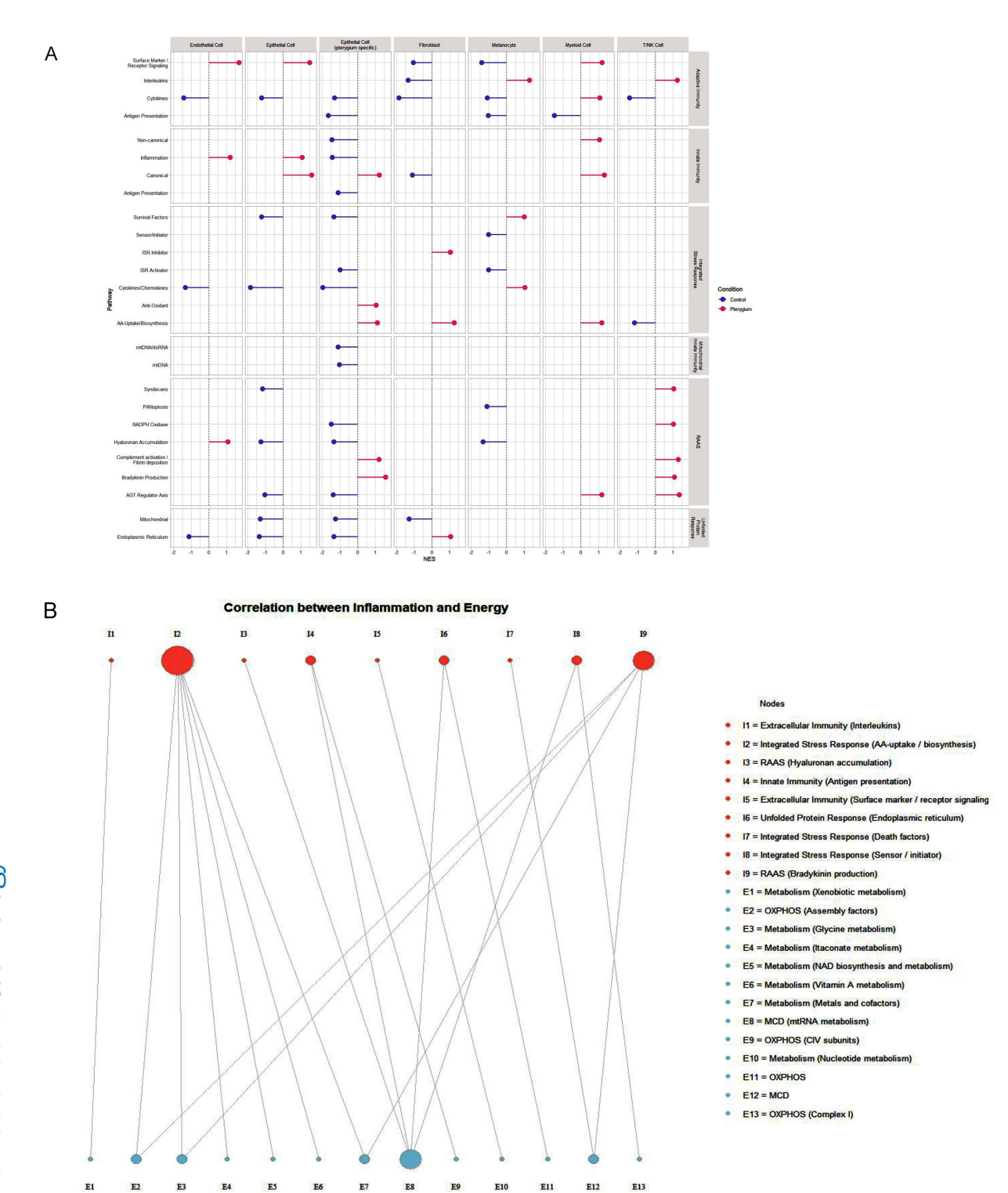


Figure 4. (A) Lollipop plot displaying NES values (|NES| > 1) of inflammatory modules for each cell type. (B) Correlation between inflammatory (pink) and mitochondrial energy metabolism-associated (blue) pathways.

reactions, and molybdenum cofactor synthesis and proteins. The modules upregulated in the T/NK cells of pterygium samples included cholesterol, bile acid, steroid synthesis, catechol metabolism, xenobi-

otic metabolism, and tetrahydrobiopterin synthesis. Endothelial cells and epithelial cells (excluding pterygium-specific epithelial cells) were mostly downregulated except for kynurenine metabolism.

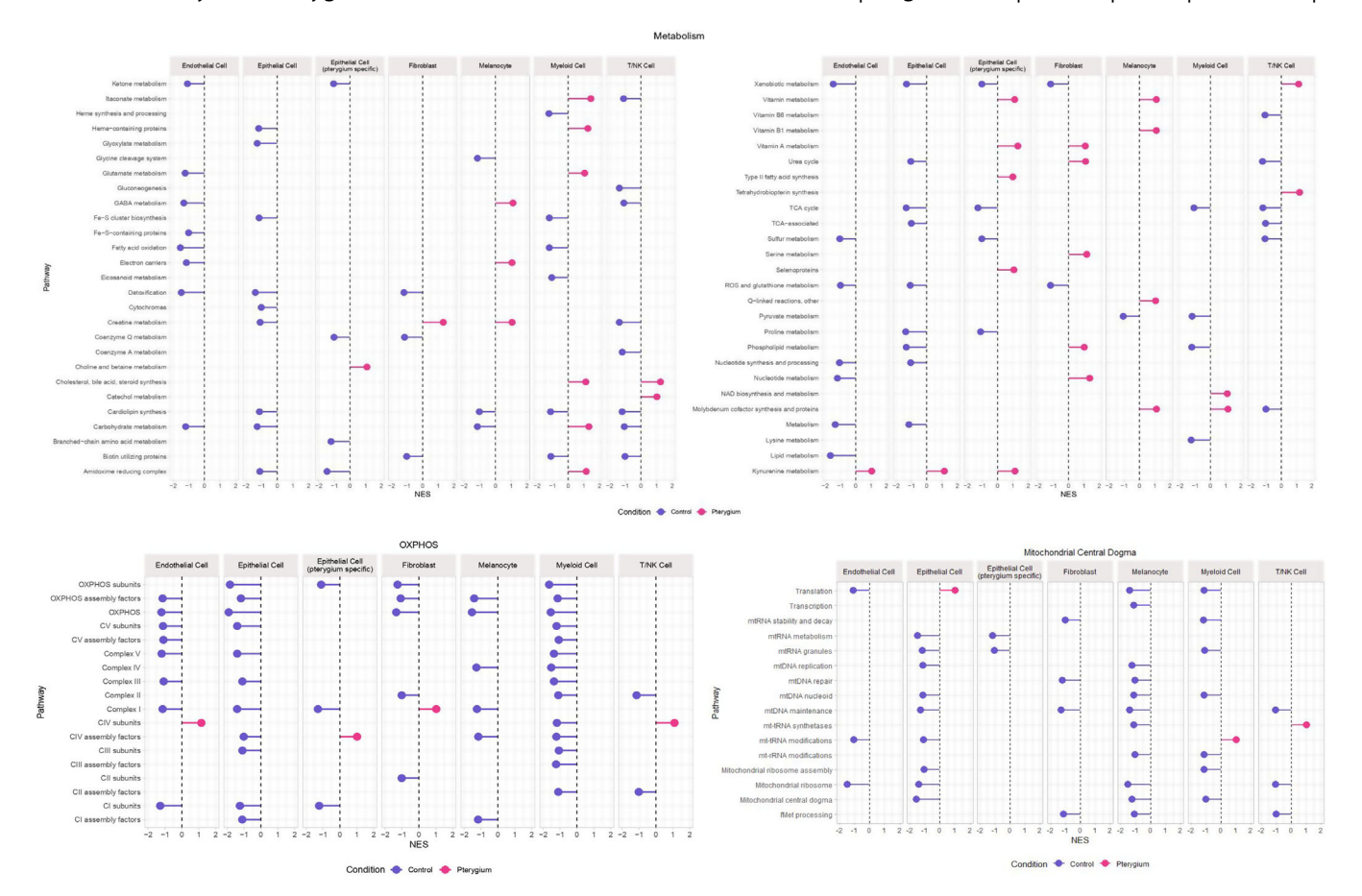


Figure 5. Lollipop plots displaying NES values (|NES| > 1) of metabolism, OXPHOS, and MCD pathways of each cell type.

Among the OXPHOS modules, the Complex IV subunits in the endothelial cells, Complex IV assembly factors in the pterygium-specific epithelial cells, Complex I in fibroblasts, and Complex IV subunits in T/NK cells were upregulated in pterygium. Among the MCD modules, translation in epithelial cells, mt-tRNA modification in myeloid cells, and mt-tRNA synthetases in T/NK cells were upregulated.

We also examined the expressions of the specific genes involved. Pterygium-specific epithelial cells demonstrated the most alterations (Figs. 6A, 6B). Inflammatory genes significantly upregulated in pterygium-specific epithelial cells contain: (i) STAT1 and DDX60, which act in sustained proinflammatory responses <sup>17,18</sup>; (ii) FAS, which actively remove damaged cells, a process likely driven by chronic inflammation <sup>19</sup>; (iii) SLC7A11 and NQO1, implicated in antioxidant defenses <sup>20,21</sup>; (iv) BDKRB1 and BDKRB2, which encode bradykinin receptors and are involved in the inflammatory environment; (v) THBD and SDC1, associated with ongoing tissue repair and remodeling. <sup>22</sup> Downregulated genes include: (i)

CX3CL1, CSF3, IL6, and CXCL8, which suggest an overall impairment in immune cell recruitment<sup>23,24</sup>; (ii) PPARGC1A and SOD2, which support mitochondrial dysfunction (Fig. 6A).<sup>25</sup>

Significantly upregulated genes associated with mitochondrial energy metabolism include: (i) PKM, ENO1, and LDHA, which reflect a shift toward aerobic glycolysis<sup>26</sup>; (ii) ALDH1L2 and TKT, which are involved in the pentose phosphate pathway<sup>27</sup>; (iii) SOD1, which mitigates oxidative damage in the cytoplasm. Significantly downregulated genes involved in mitochondrial energy metabolism contain: (i) FBP1 and SLC16A3, which are a gluconeogenic enzyme and a lactate transporter, respectively, suggesting an increased reliance of cells on glycolysis<sup>28,29</sup>; (ii) SOD2, which is a mitochondrial superoxide dismutase, further confirming mitochondrial dysfunction (Fig. 6B).<sup>30</sup>

Other cell types also appeared to contribute to the pathogenesis of pterygium. For instance, GDF15, known to modulate inflammation and promote tissue repair, was upregulated in fibroblasts. However, the downregulation of CXCL12 and CCL8 in fibroblasts



Figure 6. (A) Heatmaps of inflammatory-associated genes and (B) Heatmaps of mitochondrial energy metabolism-associated genes. Wald statistics show upregulation (*red*) and downregulation (*blue*) of gene expressions.

suggests a reduced capacity for immune cell recruitment, potentially perpetuating unresolved inflammation. Because CXCL12 regulates cell trafficking and immune responses, its downregulation could contribute to impaired tissue repair and persistent inflammation.<sup>31</sup>

In T/NK cells, the upregulation of oxidative stress response genes, including NQO1, HSPE1, and HSPD1, indicates an adaptive response by these immune cells to mitigate oxidative damage within the pterygium microenvironment. The upregulation of HSPE1 and HSPD1, which prevent protein misfolding and maintain mitochondrial proteostasis, suggests that immune cells are under significant oxidative stress, leading to a reliance on these proteins to maintain mitochondrial integrity and mitigate the effects of chronic stress.<sup>32</sup>

## **Discussion**

Multiomics approaches powered by computational analysis are vital for addressing complex biomedical research questions. While such strategies are highly valuable, the selection of appropriate pathological regions remains critical for deriving clinically meaningful insights. In pterygium, the Main region—comprising the cap, head, and neck—is a principal site of inflammatory activity and direct corneal invasion, making it a key pathological focus. Surgical removal has traditionally targeted this region; however, emerging evidence suggests that including the body and tail (accessory region) in excision may help reduce recurrence and improve cosmetic outcomes, and this practice is increasingly adopted in clinical settings. 32,33

In this study, we separated the Main and Accessory regions of pterygium and identified significant differences in their transcriptional profiles. The Accessory region was clearly distinguishable from both the Main region and normal conjunctival tissue in principal component analysis, and subsequent gene set analysis confirmed distinct molecular signatures for each compartment. These findings underscore the importance of anatomical precision in the molecular characterization of pterygium and highlight the potential clinical relevance of region-specific profiling.

To further investigate the transcriptomic profiles between Main and Normal, we used dissociationbased single-cell omics technologies that characterize cellular identities and tissue states, enabling us to examine the molecular and cellular landscape in patient-matched selective pterygium samples. Based on the differences in transcriptional profiles within the anatomical regions of pterygium, we selectively collected the Main samples for scRNA-seq to represent pterygium. Cell clustering revealed a group of epithelial cells that were highly involved in the pathology of pterygium. Using CellChat, we observed that these cells were involved in the ANGPTL, IL-1, and KLK signaling pathways. The ANGPTL pathway regulates angiogenesis, cell migration, and inflammation.<sup>34</sup> Specifically, ANGPTL4, expressed in the conjunctival epithelium of surgically excised pterygia, acts as a secondary HIF-regulated angiogenic mediator.<sup>35</sup> The IL-1 signaling pathway regulates inflammation, immune activity, and host defense, with studies showing overexpression of IL-1 in pterygium compared to normal conjunctiva.<sup>36</sup> KLKs activate proteases, growth factors, and cytokines, playing critical roles in cancer and skin disorders.<sup>37</sup> This suggests that the pterygium-specific epithelial cells found in this study are strongly associated with the immune alterations of pterygium identified in prior studies.

explore the energy-associated functional mechanisms potentially contributing to the upregulation of inflammatory modules, we assessed the association between inflammatory and mitochondrial energy metabolism-associated modules. AAuptake/biosynthesis in the ISR and bradykinin production in the RAAS displayed the highest correlation with the energy metabolism-associated modules, suggesting that the two supply considerable energy in pterygium. The two modules were mainly increased in the pterygium-specific epithelial cells, matching our hypothesis that the cell group plays a major role in the expression of pterygium. Among those with significant correlations with the inflammatory modules, pterygium expression was downregulated in OXPHOS and MCD and upregulated in metabolic pathways, suggesting a metabolic reprogramming towards metabolic pathways in pterygium.

We also found the most significantly altered genes present within pterygium-specific epithelial cells. They demonstrated an upregulation of key proinflammatory and stress-associated genes. Specifically, STAT1 and DDX60 were significantly elevated. STAT1 is critical in immune responses, where its activation leads to the transcription of genes involved in immune signaling, apoptosis, and stress responses. This contributes to a proinflammatory environment and potential immune activation, reflecting chronic exposure to stressors like UV radiation.

Moreover, the increased expression of SLC7A11 and NQO1, both involved in antioxidant defense mechanisms, suggests that pterygium-specific epithelial cells are experiencing oxidative stress, possibly triggered by chronic UV exposure. The upregulation of SLC7A11, which maintains the cellular redox environment by promoting glutathione production, indicates a heightened prerequisite for antioxidant defenses in response to chronic oxidative stress. <sup>17</sup> NQO1 detoxifies reactive quinones and reduces reactive oxygen species (ROS), underscoring the oxidative stress response. <sup>21</sup> The upregulation of these gene expressions underscores the cellular response to oxidative damage in pterygium, a critical factor contributing to chronic inflammation and aberrant tissue remodeling. <sup>38</sup>

The increased expression of BDKRB1 and BDKRB2 suggests an inflammatory environment in pterygium caused by promoting vascular permeability, pain, and tissue swelling. Furthermore, the expression of THBD and SDC1 indicates active tissue repair and remodeling. As SDC1 is critical in wound healing, its upregulation highlights its involvement in the characteristic fibrotic processes observed in pterygium.<sup>22</sup>

Conversely, the downregulation of CX3CL1, CSF3, IL6, and CXCL8 suggests an overall impairment in immune responses, potentially contributing to chronic inflammation. CX3CL1 mediates leukocyte adhesion and the recruitment of immune cell subpopulations. Its downregulation reflects impaired immune cell recruitment and adhesion, which may perpetuate inflammation in pterygium tissues.<sup>23</sup> CSF3 promotes neutrophil survival and differentiation, leading to a diminished capacity for immune surveillance and tissue repair when reduced in expression.<sup>24</sup> This likely contributes to persistent inflammation and reduced tissue repair, creating a permissive environment for the progression of pterygium.

The downregulation of mitochondrial energy metabolism-associated genes such as PPARGC1A (PGC- $1\alpha$ ) and SOD2 further supports mitochondrial

dysfunction. The downregulation of PGC- $1\alpha$ , which is critical for maintaining mitochondrial functions and detoxifying ROS, exacerbates oxidative stress, potentially explaining the mitochondrial dysfunction and inflammatory responses found in pterygium-specific epithelial cells.<sup>25</sup>

The findings of this study have significant clinical implications. Pterygium-specific epithelial cells found in the pterygium head deserve special attention, because they may be the chief drivers of corneal invasion. They likely correspond to the cells seen in Fuchs flecks, <sup>39</sup> one of the earliest histologic signs of UV damage. Similar "pterygium cells" have been described previously, 40 and their pivotal role in sustaining local inflammation provides fresh insight into disease pathogenesis. Overall, the data reinforce the view that pterygium is propelled by altered epithelial cells rather than by Tenon's capsule fibroblasts. That distinction matters because although one widely used surgical technique calls for broad Tenon's excision, 41 procedures that preserve Tenon's achieve comparable success rates. Therefore, based on these findings, this study is of great significance, because it may establish a new standard for the extent of excision in pterygium surgery, potentially improving surgical outcomes and reducing recurrence rates.

The limitations of this study include its small sample size, cross-sectional design, and the lack of integration of metabolomic data. Because there are only n = 6 for our bulk RNA-seg and n = 2 for our scRNA-seg data, future studies involving larger cohorts are necessary to overcome the limited statistical power and generalizability of our findings. Also, because of the crosssectional nature, it remains unclear how the identified transcriptomic signatures relate to clinical outcomes such as disease progression, recurrence risk, or treatment response. Future longitudinal studies incorporating serial sampling and clinical follow-up will be essential to clarify these associations. Additional in vitro experiments are also required to confirm the presence of pterygium-specific epithelial cells and the functional roles of the inflammatory biomarkers identified. For instance, quantitative polymerase chain reaction or immunohistochemistry can be used on pterygium and control tissues to compare the expression of genes found in this study.

Furthermore, although mitochondrial energy metabolism pathways were significantly correlated with inflammation in our analysis, a direct assessment through metabolomics would substantially enhance the biological relevance and mechanistic interpretation of these findings. The integration of metabolomic data—particularly focusing on mitochondrial and inflammation-related metabolic pathways—could

provide a more comprehensive understanding of disease pathogenesis and complement the transcriptomic and proteomic analyses performed in this study. Because of the lack of available metabolomic datasets from pterygium tissue, this aspect could not be addressed in the current study; however, we propose that future studies incorporate metabolomic profiling or metabolic flux analysis to validate and extend our multiomics findings.

#### **Acknowledgments**

Supported by the National Research Foundation of Korea (NRF) grants funded by the Korean government (MSIT) (RS-2022-NR070587).

Disclosure: C. Song, None; S. Myung, None; H. Cho, None; T.G. Kim, None; S. Chun, None; M. Seo, None; H. Yu, None; S. Kim, None; Y-A. Kim, None; J. Kim, None; J. Shin, None; S. Bae, None; Y. Lee, None; M.S. Kang, None; M.S. Kim, None

\* CS, SM, and HC contributed equally to this work.

## References

- Džunić B, Jovanović P, Veselinović D, Petrović A, Stefanović I, Kovačević I. Analysis of pathohistological characteristics of pterygium. *Bosn J Basic Med Sci.* 2010;10:307–313.
- 2. Chui J, Coroneo M, Lien T, Crouch R, Wakefield D, Girolamo N. Ophthalmic pterygium: a stem cell disorder with premalignant features. *Am J Pathol*. 2011;178(2):817–827.
- 3. Kim YA, Choi Y, Kim TG, et al. Multi-system-level analysis with RNA-seq on pterygium inflammation discovers association between inflammatory responses, oxidative stress, and oxidative phosphorylation. *Int J Mol Sci.* 2024;25:4789.
- 4. Ghiasian L, Samavat B, Hadi Y, Arbab M, Abolfathzadeh N. Recurrent pterygium. *J Curr Ophthalmol*. 2021;33:367–378.
- 5. Zhang Q, Bao N, Liang K, Tao L. Adjuvant use of cyclosporine A in the treatment of primary pterygium: a systematic review and meta-analysis. *Cornea*. 2018;37:1000–1007.
- 6. Arici C, Usta G. The effect of cyclosporine A in pterygium surgery using fibrin glue. *Int Ophthalmol.* 2024;44:297.
- 7. Shahraki T, Arabi A, Feizi S. Pterygium: an update on pathophysiology, clinical features,

- and Management. *Ther Adv Ophthalmol*. 2021;13:25158414211020152.
- 8. Akbari M. Update on overview of pterygium and its surgical management. *J Popul Ther Clin Pharmacol*. 2022;29(4):e30–e45.
- 9. Cloud analysis. 10x Genomics. Available at: https://www.10xgenomics.com/support/software/cloud-analysis/latest. Accessed September 15, 2024.
- 10. Zhang X, Han P, Qiu J, et al. Single-cell RNA sequencing reveals the complex cellular niche of pterygium. *Ocular Surf*. 2024;32:91–103.
- 11. Topper MJ, Guarnieri JW, Haltom JA, et al. Lethal covid-19 associates with Raas-induced inflammation for multiple organ damage including mediastinal lymph nodes. *PNAS*. 2023;121(49):e2401968121.
- 12. Guarnieri JW, Dybas JM, Fazelinia H, et al. Core mitochondrial genes are down-regulated during SARS-CoV-2 infection of rodent and human hosts. *Sci Transl Med.* 2023;15(708): eabq1533.
- 13. Wolf J, Hajdu RI, Boneva S, et al. Characterization of the cellular microenvironment and novel specific biomarkers in Pterygia using RNA sequencing. *Front Med.* 2022;8:714458.
- 14. Patergnani S, Bouhamida E, Leo S, Pinton P, Rimessi A. Mitochondrial oxidative stress and "mito-inflammation": actors in the diseases. *Biomedicines*. 2021;9:216.
- 15. Ransy C, Vaz C, Lombès A, Bouillaud F. Use of H2O2 to cause oxidative stress, the catalase issue. *Int J Mol. Sci.* 2020;21:9149.
- 16. Wilkinson-Berka JL, Suphapimol V, Jerome JR, Deliyanti D, Allingham MJ. Angiotensin II and aldosterone in retinal vasculopathy and inflammation. *Exp Eye Res.* 2019;187:107766.
- 17. Tolomeo M, Cavalli A, Cascio A. STAT1 and its crucial role in the control of viral infections. *Int J Mol. Sci.* 2022;23:4095.
- Miyashita M, Oshiumi H, Matsumoto M, Seya T. DDX60, a DEXD/H box helicase, is a novel antiviral factor promoting rig-i-like receptormediated signaling. *Mol Cell Biol.* 2011;31:3802– 3819.
- 19. Strasser A, Jost PJ., Nagata S. The many roles of Fas receptor signaling in the immune system. *Immunity*. 2009;30:180–192.
- 20. Hu K, Li K, Lv J, et al. Suppression of the SLC7A11/glutathione axis causes synthetic lethality in kras-mutant lung adenocarcinoma. *J Clin Invest*. 2020;130:1752–1766.
- 21. Ross D, Siegel D. The diverse functionality of NQO1 and its roles in redox control. *Redox Biol*. 2021;41:101950.

- 22. Stepp MA, Pal-Ghosh S, Tadvalkar G, Pajoohesh-Ganji A. Syndecan-1 and its expanding list of contacts. *Adv Wound Care*. 2015;4:235–249.
- 23. Rivas-Fuentes S, Salgado-Aguayo A, Arratia-Quijada J, Gorocica-Rosete P. Regulation and biological functions of the CX3CL1-CX3CR1 axis and its relevance in solid cancer: A mini-review. *J Cancer.* 2021;12:571–583.
- 24. Garg B, Mehta HM, Wang B, Kamel R, Horwitz MS, Corey SJ. Inducible expression of a disease-associated ELANE mutation impairs granulocytic differentiation, without eliciting an unfolded protein response. *J Biol Chem.* 2020;295:7492–7500.
- 25. Rius-Pérez S, Torres-Cuevas I, Millán I, Ortega ÁL, Pérez S. PGC-1a, inflammation, and oxidative stress: an integrative view in metabolism. *Oxid Med Cell Longev*. 2020;2020:1–20.
- 26. Zhang Z, Deng X, Liu Y, Liu Y, Sun L, Chen F. PKM2, function and expression and regulation. *Cell Biosci.* 2019;9:52.
- 27. Kim Y, Kim EY, Seo YM, Yoon TK, Lee WS, Lee KA. Function of the pentose phosphate pathway and its key enzyme, transketolase, in the regulation of the meiotic cell cycle in oocytes. *Clin Exp Reprod Med.* 2012;39(2):58.
- 28. Park HJ, Jang HR, Park SY, Kim YB, Lee HY, Choi CS. The essential role of fructose-1,6-bisphosphatase 2 enzyme in thermal homeostasis upon cold stress. *Exp Mol Med.* 2020;52:485–496.
- 29. Tao Q, Li X, Zhu T, et al. Lactate transporter SLC16A3 (MCT4) as an onco-immunological biomarker associating tumor microenvironment and immune responses in lung cancer. *Int J Gen Med.* 2022;15:4465–4474.
- 30. Flynn JM, Melov S. SOD2 in mitochondrial dysfunction and neurodegeneration. *Free Radic Biol Med.* 2013;62:4–12.
- 31. Mezzapelle R, Leo M, Caprioglio F, et al. CXCR4/CXCL12 activities in the tumor microenvironment and implications for tumor immunotherapy. *Cancers*. 2022;14:2314.
- 32. Yeung N, Murata D, Iijima M, Sesaki H. Role of human HSPE1 for OPA1 processing independent of HSPD1. *iScience*, 2023;26(2):106067.
- 33. Khandelwal R, Tigga M, Metri R, Deshpande A. Comparative study of pterygium excision with suture and sutureless conjunctival autograft. *Eur J Clin Exp Med*. 2024;22:334–339.
- 34. Lee B, Ip M, Tat L, Chen H, Coroneo M. Modified Limbal-Conjunctival Autograft Surgical Technique: Long-Term Results of Recurrence and Complications. *Cornea*. 2023;42:1320–1326.

- 35. Carbone C, Piro G, Merz V, et al. Angiopoietinlike proteins in angiogenesis, inflammation and cancer. *Int J Mol Sci.* 2018;19:431.
- 36. Meng Q, Qin Y, Deshpande M, et al. Hypoxiainducible factor-dependent expression of angiopoietin-like 4 by conjunctival epithelial cells promotes the angiogenic phenotype of pterygia. *Invest Ophthalmol Vis Sci.* 2017;58:4514–4523.
- 37. Zhou WP, Zhu YF, Zhang B, Qiu WY, Yao YF. The role of ultraviolet radiation in the pathogenesis of pterygia (Review). *Mol Med Rep.* 2016;14:3–15.
- 38. Suarez MF, Echenique J, López JM, et al. Transcriptome analysis of pterygium and Pinguec-

- ula reveals evidence of genomic instability associated with chronic inflammation. *Int J Mol Sci.* 2021;22:12090.
- 39. Ip MH, Chui JJY, Tat LT, Coroneo MT. Significance of Fuchs flecks in patients with pterygium/pinguecula: earliest indicator of ultraviolet light damage. *Cornea*. 2015;34:1560–1563.
- 40. Dushku N, John MK, Schultz GS, Reid TW. Pterygia pathogenesis: corneal invasion by matrix metalloproteinase expressing altered limbal epithelial basal cells. *Arch Ophthalmol*. 2001;119:695–706.
- 41. Hirst LW. Long-term results of P.E.R.F.E.C.T. for pterygium. *Cornea*. 2021;40:1141–1146.